EFFECT OF PARTICLE GRADATION ON SEEPAGE FAILURE IN GRANULAR SOILS

Takaji KOKUSHO[1] and Yusuke FUJIKURA[2]

[1]Member of ISSMGE, Professor, Civil Engineering Department, Chuo University
(13-27, Kasuga1, Bunkyo-ku, Tokyo, 112-8551, Japan)
E-mail: kokusho@civil.chuo-u.ac.jp
[2]Member of JSCE, Technology Development Division, Fujita Corporation
(2025-1, Ono, Atsugi City, Kanagawa, 243-0125, Japan)
E-mail:yfujikura@fujita.co.jp

By employing a large-diameter constant-head seepage test apparatus, internal instability in sand and gravel by upward water flow was investigated. Reconstituted granular soils having various particle gradations, densities and particle roundness were tested. It was found that the maximum critical hydraulic gradient for seepage failure drastically increases with increasing uniformity coefficient and becomes more than 3 times higher than the theoretical value. A mode of seepage failure is different due to different particle gradations such that poorly-graded sand or gravel (C_u<4) shows global boiling failure while well-graded gravelly sand (C_u>4) undertakes local boiling and eventual separation between coarser and finer grains. Among well-graded soils, some tends to exhibit a local piping failure of finer particles at hydraulic gradient much lower than the theoretical value, which may be predicted based on particle gradation curves.

Key Words : *seepage failure, uniformity coefficient, sand, gravel, relative density, particle shape*

1. INTRODUCTION

Experimental studies on seepage failures in laboratory using reconstituted granular materials were carried out by many investigators in the past employing one-dimensional constant head seepage test apparatus. In such tests, poorly-graded uniform sands undergo boiling failure at a hydraulic gradient i almost equal to the theoretical hydraulic gradient i_{cr}. In contrast, well-graded gravelly soils containing sands and fines do not experience apparent failure until the value i greatly exceeds i_{cr} in some cases, while in other cases start to fail at a lower value than i_{cr} in the piping failure mode, in which finer particles are selectively washed out[1), 2), 3)]. Thus, several previous researches already demonstrated that granular soils tend to exhibit different failure modes depending on particle gradation and density. However, it seems necessary to investigate by a number of systematically programmed tests how the failure modes and the critical hydraulic gradients are correlated to various physical properties of granular soils, such as soil particle gradation, relative density and particle shape.

In this research, a test program is undertaken using a large-diameter constant-head permeability test apparatus in which sandy and gravelly reconstituted specimens are tested by upward water flow to observe processes of developing seepage instability. Critical hydraulic gradients and associated failure modes of tested soils are investigated with respect to the soil particle properties to have an overview on seepage instability which may occur in granular soils.

2. TEST APPARUTUS AND SOIL MATERIALS

The constant-head seepage test apparatus shown in **Fig. 1** was used, in which the water head can be varied step by step[4)]. The size of the soil specimen in

an acrylic tube is 200 mm in diameter and 400 mm high. Water of constant head supplied from an upper tank permeates upward from the bottom to the top of the tube, and particle movements of the specimen side can be observed through the transparent tube wall. The bottom of the specimen consists of an acrylic perforated plate, a metal mesh and a paper filter and the top is covered with a metal mesh, too. The water heads within the specimen are measured with stand-pipe piezometers at 5 levels of the tube, 85 mm apart to each other. The hydraulic gradient averaged between the top of the specimen and the individual piezometers at 5 levels was used to correlate to seepage velocity calculated from the flow rate. The applied water head was increased step by step by the increment of 5 cm with the time interval of 20 to 30 minutes, and at each step any change in the specimen was carefully observed.

Soil materials tested were reconstituted basically from fluvial sand and gravel of Tone river (here represented by the capital T), comprising semi-round particles of hard stones (sandstone, chert, andesite, etc), to have prescribed particle gradations as depicted in **Fig. 2** and **Fig. 3**. **Fig. 2** shows systematically varied gradation curves T1 to T12, among which some share the same smallest or largest particle size with different values of uniformity coefficient C_u while the others have the same value of C_u with different mean grain size D_{50}. Also shown in the figure are the curves of Toyoura sand, TY, (clean sand, often used as standard sand in Japan, of the same gradation as T1) and Masa soil (decomposed granite) from Port Island, Kobe, where intensive liquefaction of reclaimed lands of this soil took place during the 1995 Kobe earthquake. **Fig. 3** shows another series of gradation curves from the river soil where sand (D = 0.075~2.0 mm) and gravel (D =2.0~26.5 mm) are mixed so that the gravel contents are systematically shifted stepwise from G_c=0 to 100% by 10% increment. Basic physical properties of these tested soils are tabulated in **Table 1** and **Table 2**. The uniformity coefficient $C_u = D_{60}/D_{10}$ and the curvature coefficient $C_c = D_{30}^2/(D_{10} \cdot D_{60})$ are also listed here. In **Table 1**, the properties of glass beads (GB) and crushed stones (CR) having exactly the same particle gradations as corresponding river soils (T) with the same label numbers are also listed.

The maximum and minimum void ratios, e_{max} and e_{min} listed in the tables were determined by using a mold with inside diameter of 195 mm and height of 200 mm and a mechanical vibrator [5]. **Fig. 4** shows variation of e_{max} and e_{min} versus uniformity coefficient C_u for T1 to T5 together with approximating curves, indicating a clear decreasing trend of void ratio with increasing C_u. **Fig. 5** shows

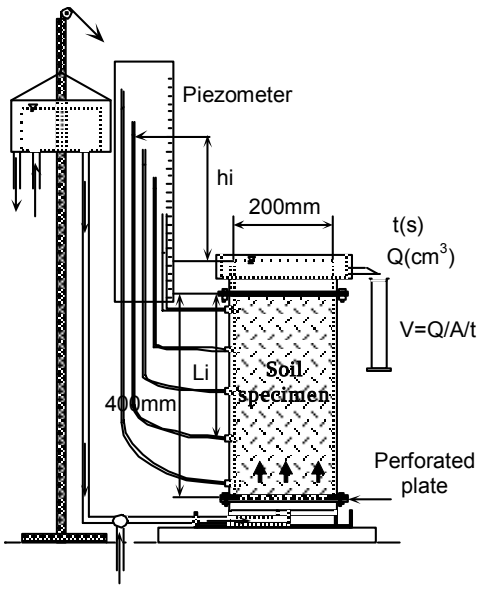

Fig.1 Constant head seepage test apparatus used in this research

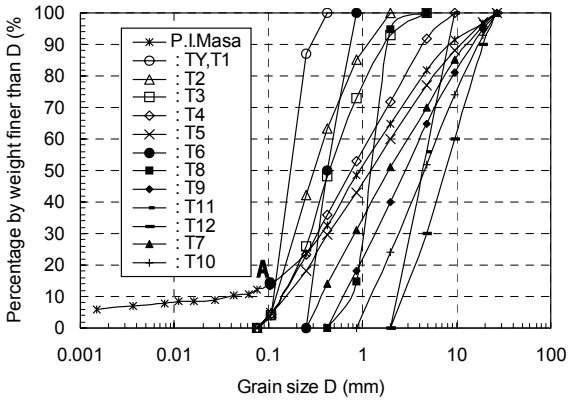

Fig.2 Grain size distribution of test materials T1~T12 and TY

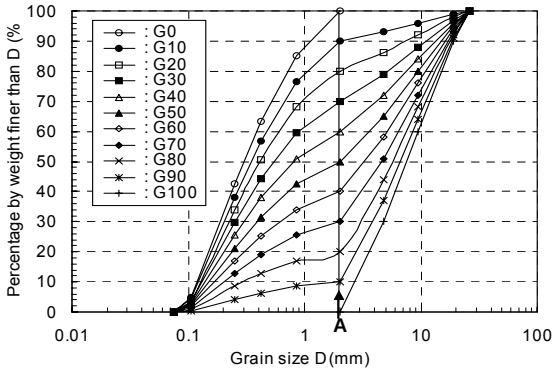

Fig.3 Grain size distribution of test materials G0~G100

the changes of e_{max} and e_{min} and C_u against the gravel content G_c for G0~G100, indicating that the void ratio approaches the minimum and the C_u-value takes the maximum at G_c=60%.

Fig. 6 shows the variation of e_{max} and e_{min} versus a grain-shape factor FU [6] for T1, TY and GB1. This

Table 1 Physical properties of soils T1~T12, TY and P.I. Masa.

Test spec.	Particle density (cm^3)	FU	e_{max}	e_{min}	Cu	Cc
TY	2.640	0.737	0.977	0.605	1.69	0.96
T1	2.696	0.671	1.250	0.795	1.69	0.96
T2	2.700	0.671	0.944	0.587	3.29	0.83
T3	2.697	0.680	0.898	0.467	4.44	0.91
T4	2.683	0.693	0.652	0.341	8.51	0.61
T5	2.655	0.707	0.585	0.303	13.60	0.59
T6	2.690	0.671	1.046	0.724	1.72	0.80
T7	2.669	0.715	0.595	0.341	8.30	0.58
T8	2.661	0.677	0.955	0.542	2.07	1.09
T9	2.649	0.733	0.516	0.320	5.55	0.77
T10	2.653	0.739	0.569	0.368	5.14	0.80
T11	2.650	0.760	0.669	0.483	2.19	0.87
T12	2.639		0.560	0.443	3.80	0.84
GB1	2.480		0.667	0.507	1.69	0.96
GB3	2.487		0.549	0.401	4.44	0.91
GB8	2.495	0.954	0.623	0.472	2.07	1.09
GB9	2.515		0.458	0.307	5.55	0.77
GB11	2.523		0.596	0.438	2.19	0.87
CR8	2.713		0.924	0.504	2.07	1.09
CR9	2.695	0.616	0.713	0.356	5.55	0.77
CR11	2.730		0.899	0.499	2.19	0.87
P.I. Masa	2.622		0.832	0.263	35.40	2.03

Table 2 Physical properties of soils G0~G100

Test specimen	Gc(%)	Particle density (cm^3)	e_{max}	e_{min}	Cu	Cc
G0	0	2.700	0.944	0.587	3.00	0.82
G10	10	2.694	0.810	0.462	3.29	0.73
G20	20	2.688	0.725	0.428	6.92	0.66
G30	30	2.682	0.655	0.389	8.46	0.51
G40	40	2.676	0.585	0.303	13.60	0.32
G50	50	2.670	0.520	0.301	23.30	0.25
G60	60	2.663	0.480	0.297	26.70	0.41
G70	70	2.657	0.445	0.312	28.60	2.74
G80	80	2.651	0.458	0.314	17.50	4.30
G90	90	2.645	0.533	0.363	4.25	0.93
G100	100	2.639	0.560	0.443	3.80	0.82

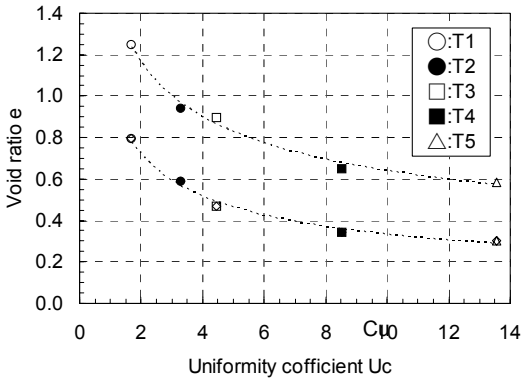

Fig.4 Relationship between C_u and e

factor can be determined as $FU=(A/s^2)/(1/4\pi)$ [6], where A and s are the area and the perimeter of the projection of a soil particle to a plane, indicating that FU tends to decrease from unity toward zero as the soil particle changes from a sphere to angular shapes. About 200 soil grains were randomly sampled in microscopic pictures of the individual soils and the FU-values were calculated as their averages. **Fig. 6** clearly demonstrates that the maximum and

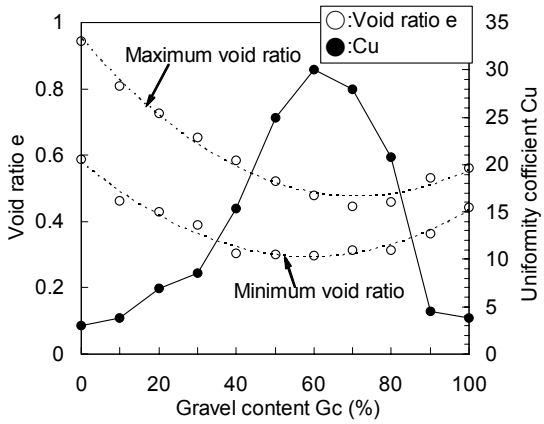

Fig.5 Relationship between G_c and e

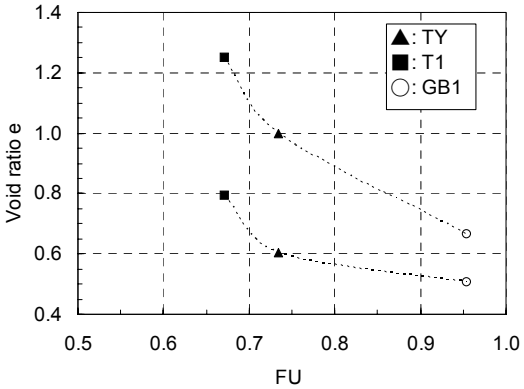

Fig.6 Relationship between FU and e

minimum void ratios are sensitive to the roundness of soil particles.

The seepage test specimen was made in the acrylic tube with prescribed densities by air-pluviation for poorly-graded sand. For gravelly soils and well-graded soils, it was prepared by a hand shovel with a great care to avoid the particle segregation and the density was controlled by tapping the tube with a wooden hammer. Then, water table was raised slowly from the bottom to saturate the specimen. Normal drinking water was used for the seepage test because a previous comparative test had demonstrated an ignorable effect of the entrained air in the water on the critical hydraulic gradient.

3. TEST RESULTS

Fig. 7 shows a seepage velocity (v) versus hydraulic gradient (i) relationship measured for poorly-graded sands T1, T2, TY and poorly-graded gravels T11, T12 having different relative density D_r. For poorly-graded sands, the seepage velocity v is almost proportional, as the Darcy's law indicates, to the hydraulic gradient i up to the end data point where an abrupt boiling failure occurs. For

poorly-graded gravels, the relationship is slightly convex as depicted in **Fig.7**, reflecting the shift from laminar flow to turbulent flow with increasing seepage velocity in highly permeable gravels. Abrupt rupture by typical boiling also occurs in gravels if they are poorly-graded. In some of medium dense to dense specimens, a kink in *i* versus *v* plots (encircled in the chart) and accompanied swelling or volume expansion can be observed just before final boiling failure both for sands and gravels.

Critical hydraulic gradient is evaluated theoretically as $i_{cr} = (\rho_s / \rho_w - 1)/(1 + e)$ where ρ_s and ρ_w are density of soil grains and water, respectively. The value i_{cr} for void ratio e between e_{max} and e_{min} are indicated with the arrow mark in **Fig. 7**. Obviously, the hydraulic gradients corresponding to the boiling failure or the swelling are mostly consistent with the theoretical gradient for the poorly-graded sandy or gravelly soils.

Fig. 8 shows a similar *v* versus *i* relationship measured for well-graded soils, T3, T4 and T5, with different values of relative density D_r. The curves are slightly winding with reverse S-shapes presumably reflecting the upward migration of finer particles and clogging the void of the upper specimen as the test continues until they reach the point of swelling encircled in the chart. Unlike poorly-graded soils, nothing occurs at or near the theoretical gradient i_{cr} shown by the arrow mark in well-graded soils with larger C_u. The specimen starts swelling at a gradient obviously higher than i_{cr} and withstand still higher gradient before ultimate failure, when a sort of particle separation takes place starting with a boiling of fine sand particles from the voids of coarse gravels. It eventually separates into two layers, finer particles above coarser particles, if the water flow is sustained still after the boiling failure. This particle separation was observed for well-graded soils of $C_u \gtrsim 4$.

Fig. 9 illustrates the *v* versus *i* relationship obtained from the test of P. I. Masa soil of 4 different relative densities containing 10% fines of low plasticity index, *Ip*=6. The fines content of 10% implies that the voids of coarser grains can accommodate all the fines, allowing the skeleton of the coarser grains to support the effective stress [2]. It undergoes local piping failure at a gradient much lower than i_{cr}, implying that fines in the voids of coarser grains are almost free from effective overburden and capable to migrate by under very low velocity flow. Then, more fierce piping failure occurs extensively under the gradient equivalent to or lower than i_{cr} depending on the difference in

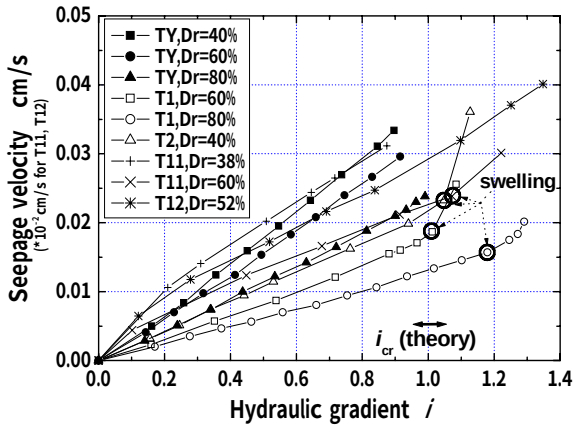

Fig.7 Hydraulic gradient versus seepage velocity for poorly-graded soils

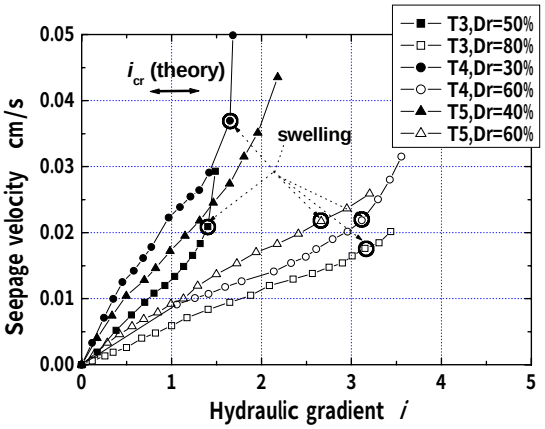

Fig.8 Hydraulic gradient versus seepage velocity for well-graded soils

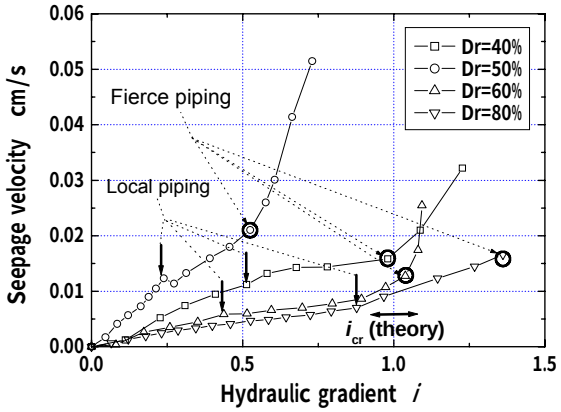

Fig.9 Hydraulic gradient versus seepage velocity for well graded decomposed granite(P. I. Masa soil).

relative density, when a great amount of finer particles are transported to the specimen surface. Based on the experimental observations, it may well be postulated that Kobe man-made islands composed of the soil underwent the similar seepage failure due to liquefaction-induced upward water flow during the 1995 Kobe earthquake, when the ground surface was actually covered with 10-20 cm of fines.

Another series of seepage tests were also carried out for the same river soils having gradation curves G0~G100 shown in **Fig. 3** to compare with the above results for the specimens T1~T12. Quite similar failure modes were again observed as the soil varies from fine sand of G0 to well-graded gravelly sand of G50 and then to poorly-graded gravel of G100; the typical boiling failure in poorly-graded sands or gravels and the swelling and the ultimate separation of sand and gravel in well-graded soils. It is also remarkable that, for the soils G80 and G90, local piping failure exclusively occurred at hydraulic gradient much lower than i_{cr}, which is very similar what happened in the P. I. Masa soil.

4. DISCUSSIONS ON SEEPAGE FAILURE OF GRANULAR SOILS

Fig. 10 shows the maximum hydraulic gradient i_{max} measured at the final stage of the seepage test and normalized by the theoretical value i_{cr} in the vertical axis plotted against the uniformity coefficient C_u in the horizontal axis for the fluvial sand and gravel (T1 to T12 and G0 to G100). The test results for 3 relative densities, D_r=30, 50 and 80%, are plotted with 3 different symbols, which are approximated by the dotted lines shown in the figure. A clear trend is obvious that the value of i_{max} drastically increases with increasing uniformity coefficient and then stays almost constant for the value of C_u higher than 10. This seems to be largely attributable to the lower void ratio or higher soil density as a result of higher uniformity coefficient as indicated in **Fig.4**. Presumably, higher density tends to cause the soil to dilate more, leading to much higher resistance to seepage failure.

In **Fig. 11**, the same experimental values (i_{max} / i_{cr}) are plotted versus the gravel content G_c and the variation may be approximated by dotted lines for relative density D_r=30, 50 and 80%, though T9 and T10 are largely deviated from the lines. It is clear from this chart that the resistance against seepage failure becomes maximum in the well-graded sandy gravel of $G_c \approx$ 50-70% and tends to decrease not only in poorly-graded sand but also in poorly-graded gravel. This seems compatible with the trend shown in **Fig.5** where the void ratio becomes minimum for the gravel content $G_c \approx$ 50-70%.

Fig. 12 depicts the normalized gradient (i_{max} / i_{cr}) versus the particle shape factor *FU* for poorly-graded soils of similar C_u-values, Toyoura sand (TY), river sand (T1), river gravel (T11), crushed stone (CR8, CR11) and glass beads (GB1 and GB8), having the same relative density of D_r=50%. A clear decreasing trend of the value (i_{max} / i_{cr}) can be recognized with increasing *FU* (roundness) of soil particles. However, the effect is not so pronounced as uniformity coefficient or relative density.

Among all the soils tested, there were three soils which underwent local piping at very low gradient; P.

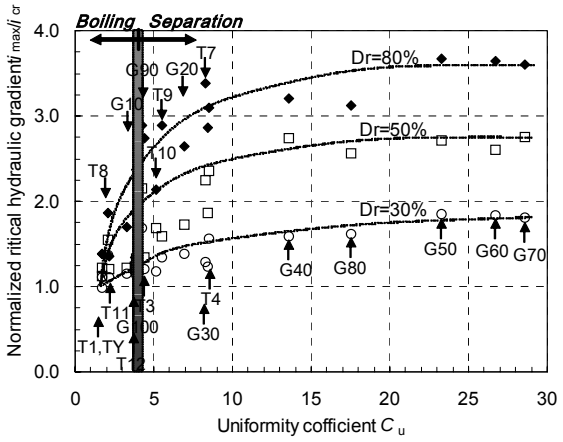

Fig.10 Relationship between uniformity coefficient and normalized maximum gradient

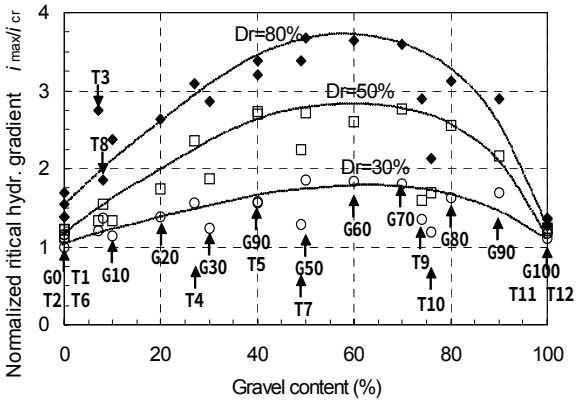

Fig.11 Relationship between gravel content and normalized maximum gradient

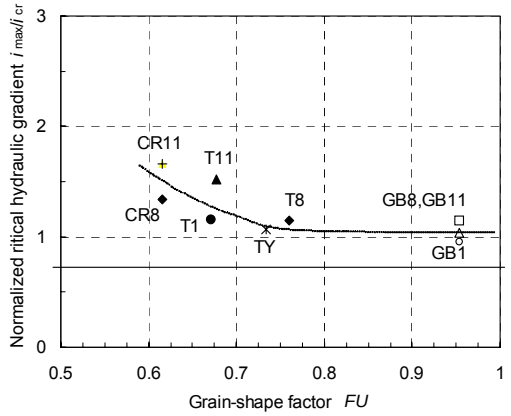

Fig.12 Relationship between grain-shape factor and normalized maximum gradient

I. Masa as depicted in **Fig.9**, G80 and G90. Note that the values of C_u of these soils are not necessarily larger than those of the rest according to **Table 1** and **Table 2**. Also note that the C_c-values of G80 and P.I. Masa is much larger than others but that of G90 is almost the same as other stable soils, while G70 with C_c larger than P. I. Masa did not occur piping. This indicates that the values of C_u and C_c may not be a proper parameter for judging piping instability.

In **Fig. 13(b)**, the gradations of the three soils (P. I. Masa, G80 and G90) are compared on F versus H chart with other soils in which no local piping was observed (G50~G70 and T5). Here, as sketched in Figure 13(a) [7], the value of F is the reading of the vertical axis (the percentage finer with the increment of 1%) for a specific particle size D, and H is that corresponding to $4D$. The line of $H = 1.3F$ on the chart is a threshold, and if the plots are above the line then the soil is stable against piping[7].

It is interesting that all the soils are crossing the threshold line and partially plotted on the instable region. However, a closer look at the chart suggests that the 3 soils in which piping actually occurred are located relatively on the left compared to the others, indicating the significance of the absolute value of F in judging the instability. A sieve test conducted after the seepage test of P. I. Masa showed that the particles transported to the surface by piping had grain size mostly finer than 0.1 mm represented by the long gentle slope of small F-values in the particle gradation curve of **Fig. 2** on the left side of the kink A. The same also holds for G90 and G80 in which a long gentle slope on the left of the kink A in **Fig. 3** represents smaller values of F combined with smaller H-values. Thus, in judging piping failures in well-graded soils based on the F versus H chart, it may be necessary to consider not only whether the F-H plots cross the threshold H=1.3F but also how small the F-value is in the unstable region.

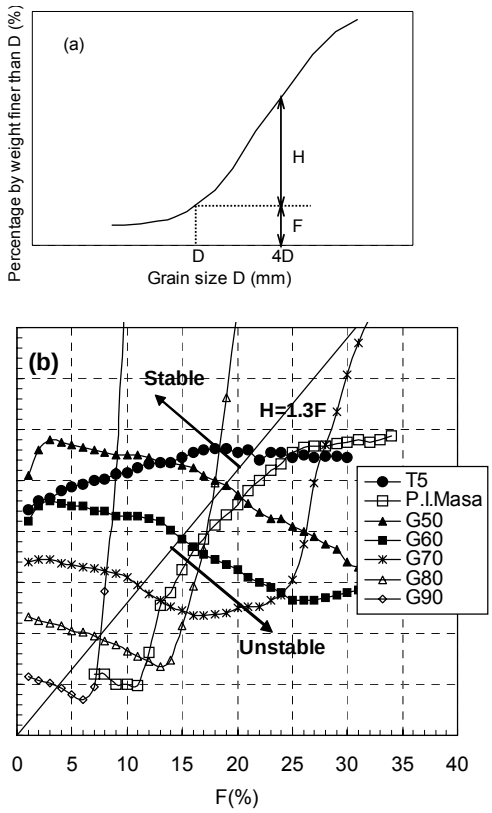

Fig.13 Definition of F and H (a) and plots of test results of 4 soils on F versus H chart (b)

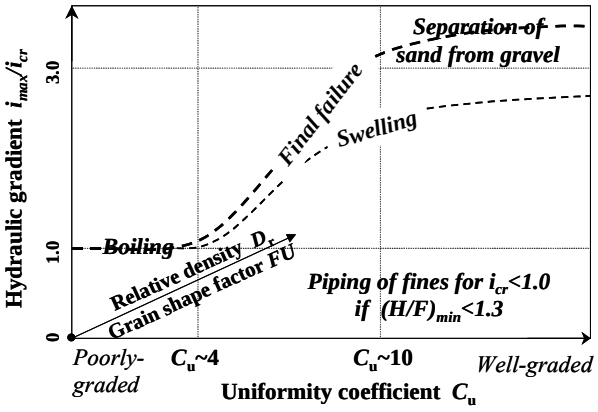

Fig.14 Overview of seepage failure in granular soils.

5. OVERVIEW OF SEEPAGE FAILURE OF GRANULAR SOILS

Based on the systematic test results, the overview of the seepage failures of granular soils may be characterized in **Fig. 14**. Without doubt, the most important parameter is particle gradation represented here by C_u. Note in **Fig 14** that the maximum hydraulic gradient i_{max} is nearly equal to the theoretical critical gradient i_{cr} in poorly-graded soils, no matter whether it is sandy or gravelly. In contrary, in well-graded soils, the maximum gradient becomes more than three times larger than the theoretical value i_{cr} particularly in dense soils. Relative density D_r also plays an important role (expressed as a third axis in **Fig. 14**) and the C_u-dependency mentioned above is intensified for larger D_r. The grain-shape factor FU (as a fourth axis) has a minor effect, decreasing the maximum gradient with increasing FU (roundness).

The final failure mode corresponding to the maximum gradient is the typical boiling failure for poorly-graded soil if it is loose in particular. In contrast, in well-graded soils of $\gtrsim 4$, remarkable swelling occurs particularly in dense soils, making the soil much more resistant against seepage failure

up to higher gradient. Then, follows eventual failure of boiling of finer soils leading to separation into sands and gravels.

Another type of failure modes for well-graded granular soils is local piping of finer soils which may occur under very low gradient if $(H/F)_{min}$<1.3 in the region of smaller F-value on the F versus H chart.

One of the major findings in this research is that the hydraulic gradient much larger than the theoretical value occurs in well-graded dense soils. All the experimental results explained above seem to support the paramount effect of void ratio on the excessively high maximum hydraulic gradient for well-graded dense soils, because higher C_u or higher FU results in higher soil density and lower void ratio as demonstrated in **Fig. 4** and **Fig.6**. Hence, initial void ratios e of individual test specimens of river soils T1~T12 and G0~G100 are plotted versus the normalized maximum gradients (i_{max} / i_{cr}) in **Fig. 15**. Fairly consistent correlation can be recognized between e and (i_{max} / i_{cr}) depending on the relative density as a parameter. Though there are significant data scatters presumably due to nonuniformity inevitably introduced in medium to loose specimens, there is little doubt that soils with e<0.4 show a high gradient of (i_{max} / i_{cr})=2.5 or larger. Thus, the absolute value of void ratio or soil density may serve as a convenient parameter in design to evaluate critical hydraulic gradient by estimating in situ relative density based on the minimum and maximum density tests.

As the dense well-graded soil start to fail, it tends to swell by the dilatancy effect, exerting large friction along the test tube wall. Thus, the high gradient can be possible only if the upward seepage force exceeding the soil weight is balanced by the friction. In the test, the lateral earth-pressure was actually measured by strain gages glued on the acrylic tube in some of the tests, which, though largely dispersed, indicated the radical increase in lateral pressure and friction along the wall during the swelling process[5].

One should be careful if such high resistance against seepage failure as in the laboratory test is applicable to actual field conditions. If the seepage occurs in a horizontal layer with a width much greater than its thickness, the excessive seepage force generated by the dilatancy effect is difficult to be supported by neighboring stable ground. The high gradient obtained in the model test seems to be realistic in situ, too, only when a specific soil layer exposed to high gradient is localized in view of the width to thickness ratio.

Finally, the above-mentioned test results are all based on reconstituted specimens, which may not reproduce some of essential in situ soil properties. Among them, cementation between particles developed by long time consolidation may have a measurable effect on seepage instability. However, the laboratory test results may be interpreted as a safer side in applying to in situ conditions.

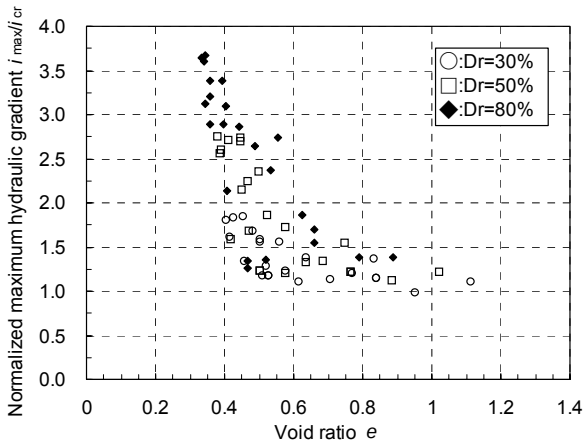

Fig.15 Void ratio versus normalized maximum hydraulic gradient for river soils T1~T12 and G0~G100.

6. CONCLUSIONS

Series of constant head seepage tests carried out for a set of granular materials with parametrically changed particle gradation curves, densities, etc. yielded the following major findings;

1) Poorly-graded loose sand tends to fail with a failure mode of typical boiling at or near the theoretical critical hydraulic gradient, while well-graded soils, if it is dense in particular, tend to exhibit swelling long before eventual failure at much high gradient.
2) The maximum hydraulic gradient i_{max} of granular soils during seepage failure is strongly dependent on their particle gradations. The normalized value (i_{max}/i_{cr}) drastically increases from unity to more than 3 with increasing uniformity coefficient up to C_u≈10. In terms of the gravel content G_c, the value (i_{max}/i_{cr}) increases to the maximum with the increase of G_c from zero to 50~70% and then decreases again as G_c approaches to 100%.
3) The roundness of soil particles have measurable effect on the maximum gradient, though the effect is minor compared to C_u.
4) The eventual failure mode shifts from global boiling in poorly-graded soils to localized boiling of finer soils in well-graded soils, which is

followed by particle separation, when the uniformity coefficient exceeds $C_u \approx 4$.

5) Finer particles contained in granular soils may migrate at a hydraulic gradient much lower than i_{cr}, leading to local piping failure, the condition of which may be identified by the plots in the unstable region for smaller F-values on the F versus H chart.
6) The normalized maximum gradient (i_{max}/i_{cr}) may be directly evaluated from void ratio based on assumed relative density, which may conveniently be used for design.
7) Although, well-graded dense soils can withstand much higher gradient than the theoretical critical gradient in the laboratory, one should be careful if the excessive seepage force can be supported by a neighboring stable soil mass in the field condition.

REFERENCES

1) Adel, H. den, Bakker, K. J. and Breteler, M.K.: Internal stability of minestone, Proc. Int. Symp. Modeling Soil-Water-Structure Interaction, Balkema , 225-231, 1988.
2) Skempton, A.W. and Brogan, J.M.: Experiments on piping in sandy gravels, Geotechnique 44, No.3, 449-460, 1994.
3) Kokusho, T., Fujikura, Y., Arai, T. and Ushiro, K.: Instability of Masa soil due to upward seepage flow, Proc., Int. Conf. on Problematic Soils, Balkema, 1998.
4) Fujikura, Y. and Kokusho, T.: Influences of soil particle gradation on seepage failure and permeability in sand and gravel, Journal of JSCE, No.687/III-56, 27-36, 2001 (in Japanese).
5) Fujikura, Y.: Seepage failure mechanism of granular soils by constant head seepage tests, MS theses, Graduate School of Chuo University, 2000 (in Japanese).
6) Yoshimura, Y. and Ogawa, S.: A simple quantification method of grain shape of granular materials such as sand, Journal of JSCE, No.463/III-22, 95-103, 1993 (in Japanese).
7) Kenney, T.C. and Lau, D.: Internal stability of granular filters, Canadian Geotech. Journal, No.22, 215-225, 1985.